

# Pump-probe diffraction imaging of vibrational wave functions

Joseph D. Geiser and Peter M. Weber

*Department of Chemistry, Brown University, Providence, Rhode Island 02912*

(Received 25 November 1997; accepted 10 February 1998)

The theory of pump-probe diffraction experiments shows that probability density distributions of vibrational wave functions are experimentally observable. In the experiment a laser prepares a molecule in a selected vibrational state, in either the same or a different electronic manifold. The diffraction pattern of the molecule in the excited state is the Fourier transform image of the nuclear probability density distribution, as determined by the vibrational eigenfunction of the molecule. This suggests the possibility to directly observe components of molecular vibrational wave functions. Model calculations illustrate the concept on iodine molecules, and sodium dimers. The relevance to time-resolved pump-probe experiments that prepare vibrational wave packets is discussed.

© 1998 American Institute of Physics. [S0021-9606(98)01119-2]

## INTRODUCTION

Diffraction experiments provide a Fourier transform image of the electron density, or charge density distribution within a molecule, a regular crystalline array, or a disordered condensed phase.<sup>1-6</sup> Using common assumptions, for example, that the electron density distributions are spherical clouds centered about an atomic nucleus,<sup>1,4,5</sup> it is possible to associate with the observed electron density distribution a specific molecular structure. In almost all diffraction experiments performed to date, the electron density distribution obtained is that of the thermal state of the system, that is, a thermal average of rotational and vibrational states. Given the dominant population of the ground vibrational level, conventional diffraction experiments are well described by taking the density distribution due to vibrational motions to be Gaussian, and including thermally excited vibrations in a classical fashion.<sup>1</sup> Similarly, gas phase experiments account for rotational distributions by averaging over all random molecular orientations.<sup>1-5</sup>

Departing from this classical approach, recent experiments by Böwering *et al.*,<sup>7,8</sup> and theory by Kohl and Shipsey,<sup>9,10</sup> as well as work done in Fink's group,<sup>11,12</sup> showed that if a molecular system is prepared in a specific rotational eigenstate, the diffraction pattern images the rotational wave function in Fourier space. The significance of this work is that individual rotational wave functions are imaged, rather than the thermal superposition of states. The concept was further developed by Ben-Nun *et al.*,<sup>13</sup> who showed that individual electronic wave functions can be imaged by both x-ray and electron diffraction. In this scheme, a diffraction pattern is observed for an atom or a molecule that is prepared in an electronically excited state by laser excitation. From this excited state pattern, a pattern of the system in the ground electronic state is subtracted. To the extent that the electronic excitation affects only a single electron, the difference between the patterns reflects the geometry of the orbital from which an electron was removed, and the orbital that received the electron. The contributions of electrons in orbitals unaffected by the laser excitation are subtracted out

in taking the difference of the diffraction patterns. Departing from conventional diffraction patterns, this pump-probe diffraction experiment images individual atomic or molecular orbitals, rather than the complete electron density of the target molecule. In contrast to the approach by Böwering, it is not necessary to prepare the entire macroscopic system in the specific eigenstate that is to be imaged. X-ray diffraction experiments on electronically excited sodium nitroprusside by Pressprich *et al.*<sup>14</sup> show that the effect of electronic excitation on diffraction patterns can in fact be quite large.

An electron diffraction pattern is the Fourier image of the Coulomb potential that is generated by the charge distribution of the molecule. The charge distribution in turn is determined by the complete atomic or molecular wave function. The concept advanced by Ben-Nun *et al.*<sup>13</sup> can therefore be generalized to include vibrational and rotational wave functions; in a pump-probe diffraction experiment, where a laser pulse transfers population from one specific electronic, vibrational or rotational state to another, the difference patterns will show the signature of all affected wave functions. In addition to the mapping of rotational states, as pursued by Böwering *et al.*, and the electronic wave functions as advanced by Ben-Nun, there exists therefore the possibility to map vibrational wave functions using diffraction techniques. Vibrational wave functions are of particular interest to chemists because chemical reactions proceed along vibrational coordinates. Moreover, the observation of vibrational wave functions in polyatomic molecules could provide a novel way to determine potential energy surfaces. It is also conceivable that pathways of vibrational energy relaxation could be observed on the level of wave functions, rather than on the level of populations, as in most spectroscopic experiments. It is therefore interesting and important to examine the effect of vibrational excitation on molecular diffraction patterns.

Recent experiments have explored the extension of pump-probe diffraction experiments into the time domain.<sup>15-48</sup> By using ultrashort pulsed laser and electron beams, a time resolution extending into the picosecond regime has been achieved.<sup>39,48</sup> It is not unreasonable to antici-

pate future diffraction experiments on the femtosecond time scale.<sup>49</sup> The theoretical descriptions of the gas phase experiments usually take the nuclear wave functions to be narrow distributions, corresponding to well-focused wave packets evolving on a steep potential energy surface.<sup>32,33,47,50–54</sup> This approach is quite reasonable if the system is prepared in the excited state by a very short laser pulse that couples a large number of eigenstates belonging to a bound or unbound surface. Many experiments that are within reach today fall short of this extreme, because they coherently couple relatively few eigenstates. The temporal evolution of the diffraction patterns in such cases is determined by the diffraction patterns of the individual eigenstates, and the temporal evolution of the amplitudes of the eigenstates. To understand time-dependent diffraction patterns of a small number of coupled states it appears important to first establish the diffraction pattern arising from an individual vibrational eigenstate. The purpose of the present paper is to begin the construction of this foundation.

Most of the formulas and calculations presented in this paper are specific to electron diffraction. Electrons are scattered off both the electron clouds and the nuclei of the target, while x-rays are scattered off only the electron density.<sup>1</sup> Within the independent atom model, the information content of electron and x-ray diffraction are the same, so that our ideas can be applied to x-ray diffraction experiments as well.

We start with a review of the theory of diffraction, and establish how it can be applied to vibrational eigenstates. Model calculations for diatomic systems with large amplitudes of vibrational motions are then presented. The specific systems we chose are molecular iodine and sodium dimers, with idealized harmonic and Morse potential surfaces. They show that the effects of the vibrational excitation on the diffraction patterns are in fact quite large. We discuss the generalization of the results to other molecular systems.

## THEORY

A suitable starting point for the analysis of pump–probe diffraction patterns is the first order expression for the inelastic scattering intensity<sup>31,55,56</sup>

$$I_{i \rightarrow f}(s) = I_{\text{cl}} |\langle \psi_f | L | \psi_i \rangle|^2, \quad (1)$$

where  $\psi_i$  is the complete wave function of the molecule in state  $i$ , and  $L$  is the scattering operator. The classical scattering intensity  $I_{\text{cl}}$  is the one derived by Rutherford,<sup>56</sup>

$$I_{\text{cl}}(s) = \left( \frac{2me}{\hbar^2 s^2} \right)^2. \quad (2)$$

Here,  $m$  is the mass of the electron with charge  $e$ , and  $s$  is the absolute value of the momentum transfer vector,  $\mathbf{s} = \mathbf{k} - \mathbf{k}_0$ . Electron diffraction is sensitive to both the nuclear and the electron charge. Therefore, the scattering operator is given by<sup>13,31,57,58</sup>

$$L = \sum_{\alpha} Z_{\alpha} e^{i\mathbf{s} \cdot \mathbf{r}_{\mathbf{n},\alpha}} - \sum_i e^{i\mathbf{s} \cdot \mathbf{r}_{\text{el},i}}, \quad (3)$$

with  $Z_{\alpha}$  the atomic number of nucleus  $\alpha$  having coordinate  $\mathbf{r}_{\mathbf{n},\alpha}$ , and  $\mathbf{r}_{\text{el},i}$  the coordinates of electron  $i$ . A similar for-

mula, with a slightly different  $I_{\text{cl}}$  and without the nuclear term, applies to x-ray scattering.<sup>13</sup> The elastic scattering event is characterized by identical initial and final states, so that the elastic scattering intensity is given by

$$I_{\text{elastic}}(s) = I_{\text{cl}} |\langle \psi_i | L | \psi_i \rangle|^2 = I_{\text{cl}} |g_{ii}(s)|^2, \quad (4)$$

where we have defined  $g_{ii}(s)$  as the elastic electron scattering amplitude of the molecule in state  $i$ . An expression for the total scattering is obtained by assuming that all final states are energetically accessible, so that the closure relation can be applied<sup>5</sup>

$$I_{\text{total}}(s) = I_{\text{cl}} \sum_f \langle \psi_i | L^* | \psi_f \rangle \langle \psi_f | L | \psi_i \rangle = I_{\text{cl}} \langle \psi_i | L^* L | \psi_i \rangle. \quad (5)$$

The integrals in Eqs. (1), (4), and (5) are over the coordinates of all nuclei and all electrons. For a polyatomic molecule with electronic and vibrational degrees of freedom, the Born–Oppenheimer approximation and the independent atom approximation are often invoked. Within the Born–Oppenheimer approximation the molecular wave function is written as the product of an electronic wave function,  $\phi(\mathbf{r}_{\mathbf{n}}, \mathbf{r}_{\text{el}})$ , and the nuclear wave function  $\chi(\mathbf{r}_{\mathbf{n}})$ ,

$$\psi(\mathbf{r}_{\mathbf{n}}, \mathbf{r}_{\text{el}}) = \phi(\mathbf{r}_{\mathbf{n}}, \mathbf{r}_{\text{el}}) \cdot \chi(\mathbf{r}_{\mathbf{n}}). \quad (6)$$

The set of coordinates  $\mathbf{r}_{\mathbf{n}}$  is conveniently the set of normal mode coordinates of the vibrational motion. The independent atom approximation associates  $Z_{\alpha}$  electrons with each nucleus. The molecule is thus modeled as a set of independent spherical atoms whose electrons move rigidly with the nuclei. It is then possible to rewrite the total wave function as a product

$$\psi(\mathbf{r}_{\mathbf{n}}, \mathbf{r}_{\text{el}}) = \phi(\mathbf{r}_{\text{el}}) \cdot \chi(\mathbf{r}_{\mathbf{n}}), \quad (7)$$

where  $\mathbf{r}_{\text{el}}$  now represents the set of coordinates  $\mathbf{r}_{\mathbf{j}\alpha}$ , which describe the position of electron  $j$  with respect to the position of the nucleus  $\alpha$  to which it belongs.<sup>17,31</sup> The electron scattering operator  $L$  may then be reexpressed in terms of the new  $\mathbf{r}_{\mathbf{j}\alpha}$ ,

$$\begin{aligned} L &= \sum_{\alpha} Z_{\alpha} e^{i\mathbf{s} \cdot \mathbf{r}_{\mathbf{n},\alpha}} - \sum_j e^{i\mathbf{s} \cdot \mathbf{r}_{\mathbf{j}\alpha}} e^{i\mathbf{s} \cdot \mathbf{r}_{\mathbf{n},\alpha}} \\ &= \sum_{\alpha} e^{i\mathbf{s} \cdot \mathbf{r}_{\mathbf{n},\alpha}} \left( Z_{\alpha} - \sum_j e^{i\mathbf{s} \cdot \mathbf{r}_{\mathbf{j}\alpha}} \right). \end{aligned} \quad (8)$$

The scattering amplitude associated with a transition of the molecule from state  $i$  to state  $f$ ,  $g_{fi}(s)$  therefore becomes

$$\begin{aligned} g_{fi}(s) &= \langle \psi_f | L | \psi_i \rangle \\ &= \langle \langle \phi_{f_e}(\mathbf{r}_{\text{el}}) \chi_f(\mathbf{r}_{\mathbf{n}}) | \sum_{\alpha} e^{i\mathbf{s} \cdot \mathbf{r}_{\mathbf{n},\alpha}} \\ &\quad \times \left( Z_{\alpha} - \sum_j e^{i\mathbf{s} \cdot \mathbf{r}_{\mathbf{j}\alpha}} \right) | \phi_{i_e}(\mathbf{r}_{\text{el}}) \chi_i(\mathbf{r}_{\mathbf{n}}) \rangle_{\text{elec}} \rangle_{\text{nuc}}, \end{aligned}$$

where the brackets indicate separate integrations over the electron and the nuclear coordinates.  $\phi_{i_e}$  and  $\phi_{f_e}$  denote the initial and final electronic states, while  $\chi_i$  and  $\chi_f$  are the initial and final vibrational states. Simplification yields

$$\begin{aligned}
g_{fi}(s) &= \langle \chi_f(\mathbf{r}_n) | \sum_{\alpha} e^{i\mathbf{s}\cdot\mathbf{r}_{n,\alpha}} \left( Z_{\alpha} \cdot \delta_{ie,fe} - \langle \phi_{fe}(\mathbf{r}_{el}) | \right. \\
&\quad \left. \times \sum_j e^{i\mathbf{s}\cdot\mathbf{r}_{j\alpha}} | \phi_{ie}(\mathbf{r}_{el}) \rangle_{\text{elec}} \right) | \chi_i(\mathbf{r}_n) \rangle_{\text{nuc}} \\
&= \langle \chi_f(\mathbf{r}_n) | \sum_{\alpha} e^{i\mathbf{s}\cdot\mathbf{r}_{n,\alpha}} (Z_{\alpha} \cdot \delta_{ie,fe} \\
&\quad - F_{\alpha}^{fi,e}(\mathbf{s})) | \chi_i(\mathbf{r}_n) \rangle_{\text{nuc}}, \quad (9)
\end{aligned}$$

where we have inserted the x-ray atomic scattering amplitude  $F_{\alpha}^{fi,e}(\mathbf{s})$ , of nucleus  $\alpha$ ,

$$F_{\alpha}^{fi,e}(\mathbf{s}) = \langle \phi_{fe}(\mathbf{r}_{el}) | \sum_j e^{i\mathbf{s}\cdot\mathbf{r}_{j\alpha}} | \phi_{ie}(\mathbf{r}_{el}) \rangle_{\text{elec}}.$$

The elastic scattering intensity immediately follows:

$$\begin{aligned}
I_{\text{elastic}}(s) &= I_{\text{cl}} \left| \langle \chi_i(\mathbf{r}_n) | \sum_{\alpha} e^{i\mathbf{s}\cdot\mathbf{r}_{n,\alpha}} (Z_{\alpha} - F_{\alpha}^{ii}(\mathbf{s})) | \chi_i(\mathbf{r}_n) \rangle_{\text{nuc}} \right|^2 \\
&= I_{\text{cl}} \left| \langle \chi_i(\mathbf{r}_n) | \sum_{\alpha} e^{i\mathbf{s}\cdot\mathbf{r}_{n,\alpha}} g_{\alpha}(s) | \chi_i(\mathbf{r}_n) \rangle_{\text{nuc}} \right|^2. \quad (10)
\end{aligned}$$

In Eq. (10) we have abbreviated the elastic electron scattering amplitude of atom  $\alpha$  as  $g_{\alpha}(s) = Z_{\alpha} - F_{\alpha}^{ii}(s)$ . A convenient expression for the total scattering intensity due to the vibrational wave function is obtained by taking the scattering process to be elastic in the electronic states, even though it may be inelastic in vibrational states. The closure relation then yields

$$\begin{aligned}
I_{\text{total}}(s) &= I_{\text{cl}} \langle \chi_i(\mathbf{r}_n) | \left| \sum_{\alpha} e^{i\mathbf{s}\cdot\mathbf{r}_{n,\alpha}} [Z_{\alpha} - F_{\alpha}^{ii}] \right|^2 | \chi_i(\mathbf{r}_n) \rangle_{\text{nuc}} \\
&= I_{\text{cl}} \langle \chi_i(\mathbf{r}_n) | \sum_{\alpha} \sum_{\beta} e^{i\mathbf{s}\cdot\mathbf{r}_{\alpha\beta}} g_{\alpha}^* g_{\beta} | \chi_i(\mathbf{r}_n) \rangle_{\text{nuc}}, \quad (11)
\end{aligned}$$

where  $\mathbf{r}_{\alpha\beta}$  is the distance vector between nuclei  $\alpha$  and  $\beta$ .

The elastic and the total electron scattering signals described by Eqs. (10) and (11), respectively, are both experimentally observable quantities.<sup>59</sup> The total signal is observed if all electrons are imaged, for example with a conventional photographic plate. The elastic signal requires rejection of all inelastically scattered electrons, e.g., by means of an energy analyzer. Bartell and Gavin pointed out that the elastic scattering signal is a one-particle property, in the sense that it measures the position  $\mathbf{r}_n$  of individual particles in the laboratory frame, while the total scattering signal depends on the separation of any two particles,  $\mathbf{r}_{\alpha\beta}$ .<sup>56</sup> The observation of the elastic scattering requires a different experimental setup than the observation of the total scattering, but it can be seen that the elastic signal measures atomic positions in a distinct way.

Formulas (10) and (11) show that the elastic and the total electron scattering signals are Fourier transforms of the spatial nuclear wave function into the  $s$ -space. Similar formulas, which omit the nuclear charge contribution, can be derived for x-ray diffraction. In most thermal systems the ground vibrational wave function is well described by a Gaussian

distribution. In this case the electron diffraction signal will also show a Gaussian distribution in  $s$ -space. If, however, the molecular sample is prepared in a specific vibrationally excited state, then the diffraction signal will be sensitively dependent on the nuclear wave function. In pump-probe diffraction experiments with vibrational excitation it is therefore important to consider the contribution of the vibrational wave function to the overall diffraction pattern.

## DIATOMIC MOLECULES

The formulas for the elastic and the total scattering involve integrals over the positions of the nuclei,  $\mathbf{r}_{n\alpha}$ , and the internuclear separations,  $\mathbf{r}_{\alpha\beta}$ , respectively. These are laboratory frame coordinates and, for a polyatomic molecule, distinct from the normal mode coordinates in which the vibrational wave functions are usually expressed. It is therefore not trivially possible to transform the normal mode vibrational wave function to obtain the vibrational diffraction pattern of polyatomic molecules. In order to illustrate our basic idea, we therefore treat the special case of a diatomic molecule. In a diatomic molecule the internuclear separation is just the normal mode coordinate, so that at least the total scattering signal can be easily obtained.

We define the internuclear separations between atom 1 and atom 2 of a diatomic molecule as

$$\begin{aligned}
\mathbf{r}_{11} &= \mathbf{r}_{22} = \mathbf{0}, \\
\mathbf{r}_{12} &= -\mathbf{r}_{21}. \quad (12)
\end{aligned}$$

The total electron scattering, Eq. (11), is then given by

$$\begin{aligned}
I_{\text{total}} &= I_{\text{cl}} [ |g_1|^2 + |g_2|^2 + g_1^* g_2 \langle \chi_i(\mathbf{r}_n) | e^{i\mathbf{s}\cdot\mathbf{r}_{12}} | \chi_i(\mathbf{r}_n) \rangle \\
&\quad + g_2^* g_1 \langle \chi_i(\mathbf{r}_n) | e^{-i\mathbf{s}\cdot\mathbf{r}_{12}} | \chi_i(\mathbf{r}_n) \rangle ]. \quad (13)
\end{aligned}$$

Making the coordinate transformation to the displacement from equilibrium coordinate,  $\xi$ , of the harmonic oscillator,

$$\xi = \mathbf{r}_{12} - \mathbf{r}_{\text{eq}}, \quad (14)$$

where  $\mathbf{r}_{\text{eq}}$  is the equilibrium internuclear distance, and expressing the vibrational wave function specifically as a function of  $\xi$  gives

$$\begin{aligned}
\frac{I_{\text{total}}}{I_{\text{cl}}} &= |g_1|^2 + |g_2|^2 + g_1^* g_2 \langle \chi_i(\xi) | e^{i\mathbf{s}\cdot\xi} | \chi_i(\xi) \rangle e^{i\mathbf{s}\cdot\mathbf{r}_{\text{eq}}} \\
&\quad + g_2^* g_1 \langle \chi_i(\xi) | e^{-i\mathbf{s}\cdot\xi} | \chi_i(\xi) \rangle e^{-i\mathbf{s}\cdot\mathbf{r}_{\text{eq}}}. \quad (15)
\end{aligned}$$

For harmonic oscillations and real atomic scattering factors (e.g., those of the first Born approximation) one obtains

$$\frac{I_{\text{total}}}{I_{\text{cl}}} = g_1^2 + g_2^2 + 2g_1g_2 \cos(\mathbf{s}\cdot\mathbf{r}_{\text{eq}}) \langle \chi_i | \cos(\mathbf{s}\cdot\xi) | \chi_i \rangle. \quad (16)$$

For homonuclear diatomic molecules this becomes

$$\frac{I_{\text{total}}}{I_{\text{cl}}g^2} = 2 + 2 \cos(\mathbf{s}\cdot\mathbf{r}_{\text{eq}}) \langle \chi_i | \cos(\mathbf{s}\cdot\xi) | \chi_i \rangle, \quad (17)$$

where the intensity on the left-hand side of the equation has been put in a form analogous to the modified molecular scattering intensity commonly used in gas phase electron

diffraction.<sup>1</sup> This emphasizes the desired signal at large  $s$ -values and provides a quantity that can be directly compared with experiments.

The case of the elastic scattering intensity is more complicated because Eq. (10) requires expression of the scattering operator in the oscillator coordinate system. We first replace the nuclear coordinates  $\mathbf{r}_{n,1}$  and  $\mathbf{r}_{n,2}$  by the center-of-mass coordinate  $\mathbf{R}$ , and the internuclear separation,  $\mathbf{r}_{12}$ ,

$$\mathbf{r}_{n,1} = \mathbf{R} + \frac{m_2}{m_1 + m_2} \mathbf{r}_{12}, \quad \mathbf{r}_{n,2} = \mathbf{R} - \frac{m_1}{m_1 + m_2} \mathbf{r}_{12}. \quad (18)$$

In the second step the internuclear separation is re-expressed by the displacement from the equilibrium coordinate, (14), eventually giving

$$\begin{aligned} \frac{I_{\text{elastic}}}{I_{\text{cl}}} &= \left| g_1 \exp \left[ i \frac{m_2}{m_1 + m_2} \mathbf{s} \cdot \mathbf{r}_{\text{eq}} \right] \right. \\ &\quad \times \langle \chi_i(\xi) | \exp \left[ i \frac{m_2}{m_1 + m_2} \mathbf{s} \cdot \xi \right] | \chi_i(\xi) \rangle_{\text{nuc}} \\ &\quad + g_2 \exp \left[ -i \frac{m_1}{m_1 + m_2} \mathbf{s} \cdot \mathbf{r}_{\text{eq}} \right] \\ &\quad \left. \times \langle \chi_i(\xi) | \exp \left[ -i \frac{m_1}{m_1 + m_2} \mathbf{s} \cdot \xi \right] | \chi_i(\xi) \rangle_{\text{nuc}} \right|^2. \end{aligned} \quad (19)$$

The expression can be simplified for harmonic potentials because of the symmetry of the wave function. If moreover the scattering factors are assumed to be real, the following formula for the elastic scattering signal is found:

$$\begin{aligned} \frac{I_{\text{elastic}}}{I_{\text{cl}}} &= g_1^2 \left| \langle \chi_i | \cos \left( \frac{m_2}{m_1 + m_2} \mathbf{s} \cdot \xi \right) | \chi_i \rangle \right|^2 \\ &\quad + g_2^2 \left| \langle \chi_i | \cos \left( \frac{m_1}{m_1 + m_2} \mathbf{s} \cdot \xi \right) | \chi_i \rangle \right|^2 \\ &\quad + 2g_1g_2 \cos(\mathbf{s} \cdot \mathbf{r}_{\text{eq}}) \langle \chi_i | \cos \left( \frac{m_2}{m_1 + m_2} \mathbf{s} \cdot \xi \right) | \chi_i \rangle \\ &\quad \cdot \langle \chi_i | \cos \left( \frac{m_1}{m_1 + m_2} \mathbf{s} \cdot \xi \right) | \chi_i \rangle. \end{aligned} \quad (20)$$

For homonuclear diatomic molecules,  $m_1 = m_2$  and  $g_1 = g_2 = g$ , so Eq. (20) reduces to

$$\frac{I_{\text{elastic}}}{I_{\text{cl}}g^2} = [2 + 2 \cos(\mathbf{s} \cdot \mathbf{r}_{\text{eq}})] \left| \langle \chi_i | \cos \left[ \frac{\mathbf{s} \cdot \xi}{2} \right] | \chi_i \rangle \right|^2. \quad (21)$$

Formulas (17) and (21) are the final results for the total and the elastic scattering of vibrational wave functions for homonuclear diatomic molecules, within the harmonic oscillator approximation. The total scattering signal features rapid oscillations due to the internuclear separation,  $\mathbf{r}_{\text{eq}}$ , modulated by the cosine transform of the vibrational wave function. The elastic scattering is also modulated by the internuclear separation. However, the cosine transform is over one half times the oscillator displacement coordinate, reflecting the fact that the transform is dependent on the individual atom position,

as measured from the center-of-mass. This is ultimately the reason why the formula for the heteronuclear diatomic molecule, Eq. (20), is so much more complex.

At very large diffraction angles the cosine transform integrals of both the elastic and the total scattering tend toward zero. At those large  $s$ -values the total observed signal is dominated by the inelastic scattering. At very small scattering angles, on the other hand, the total signal is dominated by elastic scattering. This is quite analogous to the results for scattering from electronic wave functions.<sup>56</sup>

## AN ILLUSTRATION: IODINE MOLECULES AND SODIUM DIMERS

To illustrate the effects of the vibrational wave function on electron diffraction patterns, we calculated the purely vibrational contribution to the diffraction signal for the case of two model diatomic molecules. For these calculations we chose iodine,  $\text{I}_2$ , and sodium dimers,  $\text{Na}_2$ , because of the large amplitude of their classical vibrational motions, which should give rise to a pronounced effect in the diffraction pattern. Extensions to other molecules are discussed later. To display the purely vibrational effects, we assume that the molecule is aligned with its axis parallel to the momentum transfer vector. To specifically include the effect of random orientation, or of alignment induced by a polarized pump laser, our results should be superimposed with the diffraction signature of rotational states, as calculated by Kohl and Shipsey,<sup>9,10</sup> or Williamson and Zewail.<sup>47</sup>

Figure 1 shows the vibrational contribution to the total diffraction intensity of an idealized iodine molecule, calculated using Eq. (17). The vibrational potential is taken to be harmonic, with an internuclear distance  $r_{\text{eq}}$  of 2.667 Å, and a force constant of  $k = 172.1$  N/m. These parameters approximate the iodine molecule in its ground electronic state.<sup>60</sup> For panel (1a), the wave function is that of the ground vibrational state,  $n = 0$ . The main features of the vibrational diffraction pattern are the rapid oscillations, and their modulation by a slowly decaying amplitude. Since the diffraction pattern is the Fourier transform of the wave function in real space, the two features suggest that there are two lengths scales involved in the diffraction pattern. Indeed, the rapid oscillations are due to the internuclear distance of the iodine atoms. The Gaussian decay with increasing  $s$  arises from the Gaussian envelope of the vibrational wave function. The two length scales in the molecule are therefore the internuclear distance, and the amplitude of the vibrational motion. Since the vibrational amplitude is small for the ground vibrational state, the vibrational diffraction pattern stretches to very large  $s$ -values. In conventional diffraction experiments, the decay of the diffraction intensity with increasing  $s$  is accounted for by allowing a range of internuclear distances.<sup>5,58</sup> For the  $n = 0$  level the resulting formulas are equivalent.

Note that the maximum amplitude in panel (1a) is 4, while the intensity becomes 2 in the limit of large  $s$ . To isolate the purely vibrational contributions, we divided in Eq. (17) the total scattering signal by the classical scattering intensity and the atomic scattering factor  $g(s)$ . Thus, the steep decay of the electron scattering signal with increasing  $s$  observed in diffraction experiments is excluded in Fig. 1. Ex-

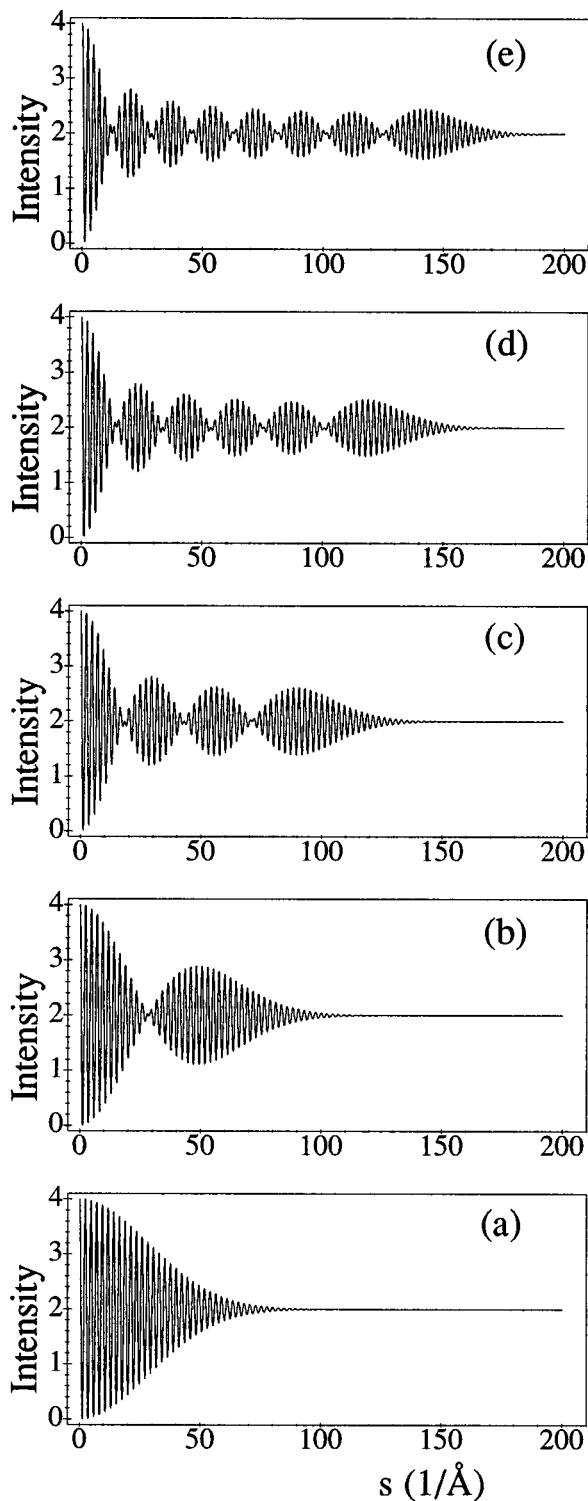


FIG. 1. The total electron scattering intensity arising from the vibrational wave function of the iodine molecule in the harmonic approximation. Panel (a) for  $n=0$ ; panel (b) for  $n=1$ ; panel (c) for  $n=3$ ; panel (d) for  $n=5$ ; and panel (e) for  $n=7$ .

perimental electron diffraction measurements account for the rapid decay by using a sector element.<sup>1</sup> The intensity scale in Fig. 1 essentially replicates the diffraction pattern observed in an experiment with a rotating sector.

Panels (b), (c), (d), and (e) of Fig. 1 show the diffraction patterns for excited vibrational states of the harmonic oscil-

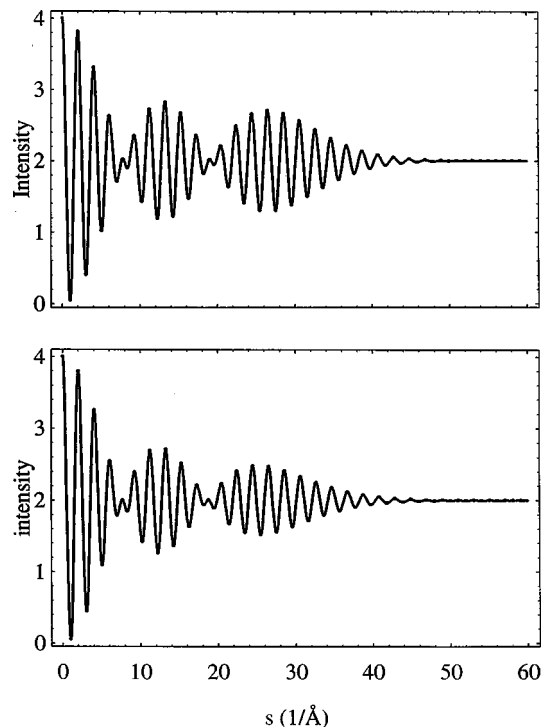


FIG. 2. The total electron scattering intensity arising from the second excited state,  $n=2$ , vibrational wave function of the idealized sodium dimer in the harmonic approximation (top panel) and the Morse approximation (bottom panel).

lator, with  $n=1, 3, 5$ , and  $7$ . In all these panels, the rapid oscillations arise from the internuclear distance, while the envelopes reflect the Fourier transforms of vibrational wave functions of the respective states. Measurement of the envelopes of the vibrational diffraction patterns therefore offers an experimental method of observing the probability density distribution of vibrational wave functions.

We point out that the conventional treatment of diffraction patterns uses a classical probability distribution for the vibrating atoms. This leads to the inclusion of a Gaussian term containing the vibrational amplitude.<sup>1</sup> Enhanced vibrational motion leads, in that approximation, to a Gaussian shaped decay of the diffraction signal, similar to Fig. 1(a), but with a more rapid decay. As can be seen from Fig. 1, such a classical treatment completely misses the modulation of the diffraction patterns for vibrationally excited states, and the components of the diffraction patterns at very large  $s$ -values.

The harmonic potential used for the calculation of the vibrational diffraction patterns of iodine can only be a crude approximation to real molecules. To explore the effect of anharmonicity we used the approximate Eq. (17) to calculate some vibrational diffraction patterns of sodium dimers in their ground electronic state. The upper panel of Fig. 2 shows the result for the harmonic potential, while the lower panel shows the situation for a Morse potential (parameters from Varshni<sup>60</sup>). Both traces are for  $n=2$  vibrational eigenstates. As expected, the anharmonicity does not change the conclusions drawn from the calculations for the harmonic iodine molecule; the diffraction pattern features a rapidly oscillating part due to the internuclear distance, and a slowly

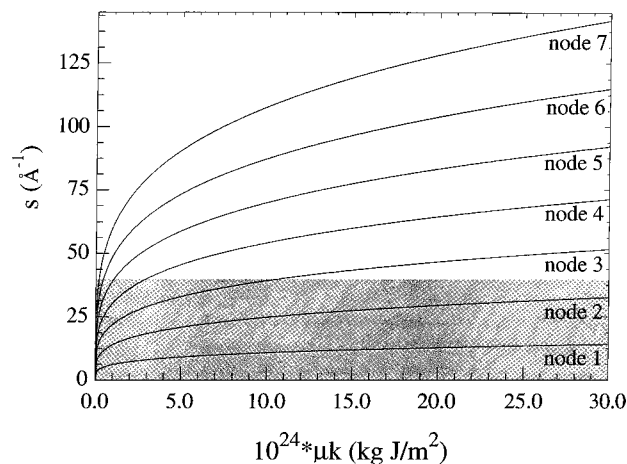


FIG. 3. Dependence of the node position for the  $n=7$  diffraction pattern on the product  $\mu \cdot k$ . The shaded area represents the portion of the  $s$ -space that is accessible by conventional diffractometers.

varying envelope that is the transform of the square of the vibrational wave function. There are a couple of notable differences between the two vibrational diffraction patterns; the pattern from the Morse oscillator dampens out quicker, reflecting the spatially more extended wave function. Also, in the vicinity of the nodes of the overall envelope, the rapid oscillations appear to be very sensitive to the exact shape of the wave function. Since the difference between the two potential functions is quite small for  $n=2$ , the fact that the diffraction pattern shows differences between them holds out the promise that potential energy surfaces may be mapped by pump-probe diffraction experiments.

## DISCUSSION

The simulated diffraction patterns shown in Figs. 1 and 2 were calculated for harmonic wells with large amplitude motion, as appropriate for the iodine molecule and the sodium dimer. Large amplitude motions likely show a large effect in the Fourier transform image of the diffraction patterns because of the inverse relation between real space and momentum space. However, even in these extreme cases the shape of the vibrational probability density distribution manifests itself at very large  $s$ -values only. The question arises if the effect under consideration is at all observable within the range of conventional diffractometers. Figure 3 shows the  $s$ -values for the nodes of the diffraction pattern corresponding to the  $n=7$  eigenstate, as a function of the product of the reduced mass,  $\mu$ , and the force constant of the potential,  $k$ . The amplitude of the harmonic vibrational motion in a diatomic molecule scales as  $1/(\mu \cdot k)^{1/4}$ . The region of  $s$ -values covered by common diffractometers is shaded in Fig. 3. It can be seen that, since most common diatomic molecules have  $\mu \cdot k$  products of less than  $30 \cdot 10^{-24}$  kg J/m<sup>2</sup>, at least two of the nodes should be observed in diffraction patterns. Molecules with large vibrational amplitudes, such as hydrogen ( $\mu \cdot k = 0.5 \cdot 10^{-24}$  kg J/m<sup>2</sup>), will show many more nodes.

Figure 4 illustrates the dependence of  $s$  on the product  $\mu \cdot k$ , for the first node in the vibrational diffraction patterns

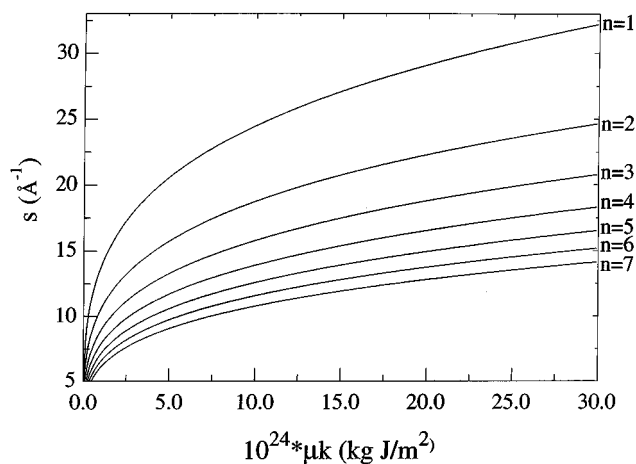


FIG. 4. The dependence of the position of the first node on the product  $\mu \cdot k$ , for vibrational diffraction patterns of states with  $n=1$  to  $n=7$ , within the harmonic approximation.

for the vibrational states from  $n=1$  to  $n=7$ . Again, within the range usually accessed by diffractometers, the first node should be observable for almost all diatomic molecules. In general, higher vibrational quantum states show nodes at smaller  $s$ -values. We conclude that the effect we describe should clearly bear signature in the diffraction patterns of most vibrationally excited diatomic molecules. We note, however, that the inversion of diffraction patterns to obtain complete images of the square of vibrational wave functions does in fact require the observation of diffraction patterns to very large scattering angles.

In gas phase diffraction experiments the molecules are typically randomly oriented. In pump-probe experiments the polarization of the laser, as well as the transition dipole moment, lead to a partial alignment of the molecular ensemble that will be reflected in the diffraction pattern.<sup>5,11,12,47,58,61,62</sup> The details of this alignment are dependent on the orientation of the transition dipole moment with respect to the axis of the molecule, the state of polarization of the laser field, and the geometry of the electron and laser beams.<sup>47</sup> In our model calculations all the alignment effects were omitted, raising the question if the effect of vibrational probability distributions might be observable in an experiment. We note that the rapid oscillations due to the internuclear separation are observed in conventional gas phase diffraction patterns; after all, it is their analysis that yields the molecular geometry. Since the envelope arising from the Fourier transform of the vibrational probability density distribution fully modulates the rapid oscillations, it is evident that the envelopes will be experimentally observable. Conventional diffraction experiments probe samples in thermal equilibria. In these experiments the majority of the molecules are in the ground vibrational state, and the effect that we describe here would be hidden. In the pump-probe diffraction experiment a sizable fraction of the molecules may be transferred to a specific excited state, making the vibrational probability density distribution observable. We note that, since an electronic excitation process may well change the internuclear distance, the diffraction oscillations from the two states involved may be

out-of-phase. In that case the amplitude of the vibrational effect may exceed the fractional excitation of the ensemble by a factor of 2.

## SUMMARY AND OUTLOOK

The theory of diffraction, as applied to electron and x-ray diffraction, suggests that the observed diffraction pattern is the Fourier transform of the molecular probability density, that is, the square of the wave functions. If molecules are selectively prepared in vibrationally excited states, then the diffraction pattern provides an image of the vibrational probability distribution. On the example of diatomic molecules we have shown that the signature of the excited state vibration is a modulation of the diffraction pattern at large  $s$ -values. For typical diatomic molecules, at least a few of the nodes should be observable within the  $s$ -range of conventional diffractometers. Extending the range of diffractometers may provide a transform image of the entire wave function, which could provide a new method of mapping potential energy surfaces. We note that the vibrational probability distributions may advantageously be observed in excited electronic states, where Franck–Condon factors to highly excited vibrational states are often favorable. Experimental work along this line is in progress.

The discussion of this paper focused on systems that are completely excited to a specific vibrational state. Most diffraction experiments within reach to date fall well short of that goal, in that only a small fraction of the molecules are prepared in an excited state. In general, the partial excitation leads to a superposition of the wave functions of the ground and the excited states, which can give rise to interesting interference effects.<sup>13,17</sup> Their influence on the vibrational diffraction patterns remains to be explored.

## ACKNOWLEDGMENTS

Acknowledgment is made to the Army Research Office (Grant No. DAAH04-96-1-0188) for financial support of this work. We greatly benefited from discussions with Professor Kent Wilson, Dr. M. Ben-Nun, Mr. R. Dudek, and Mr. Y.-H. Cheng.

- <sup>1</sup>I. Hargittai, in *Stereochemical Applications of Gas-Phase Electron Diffraction*, edited by I. Hargittai and M. Hargittai (VCH, Weinheim, 1988), pp. 1–54.
- <sup>2</sup>J. M. Cowley, in *Electron Diffraction Techniques* (Oxford University Press, New York, 1992).
- <sup>3</sup>I. Hargittai, in *Electron Diffraction Techniques*, edited by J. M. Cowley (Oxford University Press, New York, 1992), pp. 533–562.
- <sup>4</sup>R. A. Bonham and M. Fink, *High Energy Electron Scattering* (Van Nostrand Reinhold, New York, 1974).
- <sup>5</sup>J. M. Cowley, in *International Tables for Crystallography*, edited by A. J. C. Wilson (Kluwer Academic, Dordrecht, 1991), pp. 223–225.
- <sup>6</sup>J. Drenth, *Principles of Protein X-Ray Crystallography* (Springer, Berlin, 1994).
- <sup>7</sup>N. Böwering, M. Volkmer, C. Meier, J. Lieschke, and M. Fink, *Z. Phys. D* **30**, 177 (1994).
- <sup>8</sup>N. Böwering, M. Volkmer, C. Meier, J. Lieschke, and R. Dreier, *J. Mol. Struct.* **348**, 49 (1995).
- <sup>9</sup>D. A. Kohl and E. J. Shipsey, *Z. Phys. D* **24**, 33 (1992).
- <sup>10</sup>D. A. Kohl and E. J. Shipsey, *Z. Phys. D* **24**, 39 (1992).
- <sup>11</sup>M. Fink, A. W. Ross, and R. J. Fink, *Z. Phys. D* **11**, 231 (1989).
- <sup>12</sup>A. Mihill and M. Fink, *Z. Phys. D* **14**, 77 (1989).
- <sup>13</sup>M. Ben-Nun, T. J. Martinez, P. M. Weber, and K. R. Wilson, *Chem. Phys. Lett.* **262**, 405 (1996).
- <sup>14</sup>M. R. Pressprich, M. A. White, Y. Vekhter, and P. Coppens, *J. Am. Chem. Soc.* **116**, 5233 (1994).
- <sup>15</sup>M. Aeschlimann *et al.*, in *Time-Resolved Electron and X-ray Diffraction* (SPIE, San Diego, 1995), p. 103.
- <sup>16</sup>C. P. J. Barty *et al.*, in *Time-Resolved Electron and X-Ray Diffraction*, edited by P. M. Rentzepis (SPIE, San Diego, 1995), pp. 246–257.
- <sup>17</sup>C. P. J. Barty *et al.*, in *Time Resolved Electron and X-Ray Diffraction*, edited by P. M. Rentzepis and J. Helliwell (Oxford University Press, New York, 1997).
- <sup>18</sup>J. P. Bergsma, M. H. Colodonato, P. M. Edelsten, K. R. Wilson, and D. R. Fredkin, *J. Chem. Phys.* **84**, 6151 (1986).
- <sup>19</sup>P. Chen, I. V. Tomov, and P. M. Rentzepis, *J. Chem. Phys.* **104**, 10001 (1996).
- <sup>20</sup>M. Dantus, S. B. Kim, J. C. Williamson, and A. H. Zewail, *J. Phys. Chem.* **98**, 2782 (1994).
- <sup>21</sup>H. E. Elsayed-Ali, T. B. Norris, M. A. Pessot, and G. A. Mourou, *Phys. Rev. Lett.* **58**, 1212 (1987).
- <sup>22</sup>H. E. Elsayed-Ali and J. W. Herman, *Appl. Phys. Lett.* **57**, 1508 (1990).
- <sup>23</sup>H. E. Elsayed-Ali, in *Time-Resolved Electron and X-ray Diffraction*, edited by P. M. Rentzepis (SPIE, San Diego, 1995), p. 92.
- <sup>24</sup>H. E. Elsayed-Ali and P. M. Weber, in *Time Resolved Electron and X-Ray Diffraction*, edited by P. M. Rentzepis and J. Helliwell, (Oxford University Press, New York, 1997).
- <sup>25</sup>S. Erramilli, F. Osterberg, S. M. Gruner, M. W. Tate, and M. Kriechbaum, in *Time-Resolved Electron and X-Ray Diffraction*, edited by P. M. Rentzepis (SPIE, San Diego, 1995), p. 188.
- <sup>26</sup>J. D. Ewbank *et al.*, *Mol. Cryst. Liq. Cryst.* **187**, 351 (1990).
- <sup>27</sup>J. D. Ewbank *et al.*, *Rev. Sci. Instrum.* **63**, 3352 (1992).
- <sup>28</sup>J. D. Ewbank *et al.*, *J. Phys. Chem.* **97**, 8745 (1993).
- <sup>29</sup>J. D. Ewbank, L. Schäfer, and A. A. Ischenko, *J. Mol. Struct.* **321**, 265 (1994).
- <sup>30</sup>J. D. Geiser and P. M. Weber, in *Time-Resolved and X-Ray Diffraction*, edited by P. M. Rentzepis (SPIE, San Diego, 1995), p. 136.
- <sup>31</sup>J. D. Geiser, thesis, Brown University, Providence, 1998.
- <sup>32</sup>A. A. Ischenko, J. D. Ewbank, and L. Schäfer, *J. Phys. Chem.* **99**, 15790 (1995).
- <sup>33</sup>A. A. Ischenko, L. Schäfer, and J. D. Ewbank, *J. Mol. Struct.* **376**, 157 (1996).
- <sup>34</sup>B. C. Larson, C. W. White, T. S. Noggle, and D. Mills, *Phys. Rev. Lett.* **48**, 337 (1982).
- <sup>35</sup>B. C. Larson and J. Z. Tischler, in *Time-Resolved Electron and X-Ray Diffraction*, edited by P. M. Rentzepis (SPIE, San Diego, 1995), p. 208.
- <sup>36</sup>K. Moffat, in *Time-Resolved Electron and X-Ray Diffraction*, edited by P. M. Rentzepis (SPIE, San Diego, 1995), p. 182.
- <sup>37</sup>G. Mourou and S. Williamson, *Appl. Phys. Lett.* **41**, 44 (1982).
- <sup>38</sup>P. M. Rentzepis, P. Chen, and I. V. Tomov, *J. Chin. Chem. Soc.* **42**, 119 (1995).
- <sup>39</sup>T. Guo *et al.*, in *Application of High Field and Short Wavelength Sources Topical Meeting* (SPIE, Santa Fe, 1997).
- <sup>40</sup>J. R. Thompson, P. M. Weber, and P. J. Estrup, in *Time-Resolved Electron and X-Ray Diffraction*, edited by P. M. Rentzepis (SPIE, San Diego, 1995), p. 113.
- <sup>41</sup>I. V. Tomov, P. Chen, and P. M. Rentzepis, *Rev. Sci. Instrum.* **66**, 5214 (1995).
- <sup>42</sup>S. Williamson and G. Mourou, *Phys. Rev. Lett.* **52**, 2364 (1984).
- <sup>43</sup>S. Williamson and G. Mourou, in *Ultrafast Phenomena IV*, edited by D. H. Auston and K. B. Eisenthal (Springer, Berlin, 1984), p. 114.
- <sup>44</sup>J. C. Williamson and A. H. Zewail, *Proc. Natl. Acad. Sci. USA* **88**, 5021 (1991).
- <sup>45</sup>J. C. Williamson, M. Dantus, S. B. Kim, and A. H. Zewail, *Chem. Phys. Lett.* **196**, 529 (1992).
- <sup>46</sup>J. C. Williamson and A. H. Zewail, *Chem. Phys. Lett.* **209**, 10 (1993).
- <sup>47</sup>J. C. Williamson and A. H. Zewail, *J. Phys. Chem.* **98**, 2766 (1994).
- <sup>48</sup>J. C. Williamson, J. Cao, H. Ihee, H. Frey, and A. H. Zewail, *Nature (London)* **386**, 159 (1997).
- <sup>49</sup>P. M. Weber, S. D. Carpenter, and T. Lucza, in *Time-Resolved Electron and X-Ray Diffraction*, edited by P. M. Rentzepis (SPIE, San Diego, 1995), p. 23.
- <sup>50</sup>A. A. Ischenko, V. P. Spiridonov, L. Schäfer, and J. D. Ewbank, *J. Mol. Struct.* **300**, 115 (1993).
- <sup>51</sup>A. A. Ischenko, L. Schäfer, J. Y. Luo, and J. D. Ewbank, *J. Phys. Chem.* **98**, 8673 (1994).

- <sup>52</sup>A. A. Ischenko, J. D. Ewbank, and L. Schäfer, *J. Mol. Struct.* **320**, 147 (1994).
- <sup>53</sup>A. A. Ischenko, J. D. Ewbank, and L. Schäfer, *J. Phys. Chem.* **98**, 4287 (1994).
- <sup>54</sup>A. A. Ischenko, J. D. Ewbank, V. A. Lobastov, and L. Schäfer, in *Time-Resolved Electron and X-Ray Diffraction*, edited by P. M. Rentzepis (SPIE, San Diego, 1995), p. 123.
- <sup>55</sup>R. A. Bonham and J. L. Peacher, *J. Chem. Phys.* **38**, 2319 (1963).
- <sup>56</sup>L. S. Bartell and R. M. Gavin Jr., *J. Am. Chem. Soc.* **86**, 3493 (1964).
- <sup>57</sup>S. Shibata and F. Hirota, in *Stereochemical Applications of Gas-Phase Electron Diffraction*, edited by I. Hargittai and M. Hargittai (VCH, Weinheim, 1988), pp. 107–138.
- <sup>58</sup>L. S. Bartell, in *Stereochemical Applications of Gas-Phase Electron Diffraction*, edited by I. Hargittai and M. Hargittai (Chemie, New York, 1988), pp. 55–84.
- <sup>59</sup>T. Iijima, R. A. Bonham, and T. Ando, *J. Phys. Chem.* **67**, 1472 (1963).
- <sup>60</sup>Y. P. Varshni, *Rev. Mod. Phys.* **29**, 664 (1957).
- <sup>61</sup>D. A. Kohl and R. A. Bonham, *J. Chem. Phys.* **47**, 1634 (1967).
- <sup>62</sup>D. A. Kohl and L. S. Bartell, *J. Chem. Phys.* **51**, 2891 (1969).